Wavelength switching in a mixed structure of a long-period and a Bragg fiber gratings

Chih-Nan Lin (林志南), Yean-Woei Kiang (江衍偉), and C. C. Yang (楊志忠)

Graduate Institute of Communication Engineering, Graduate Institute of Electro-Optical Engineering and Department of Electrical Engineering, National Taiwan University, 1, Roosevelt Road, Section 4, Taipei

Received Novermber 1, 2002

We built a numerical model for evaluating the coupling processes of a mixed structure of a Bragg fiber grating and a long-period grating. From the numerical results, we not only confirmed the wavelength switching phenomena observed in previously reported experiments, but also discovered a new coupling mechanism, which generated the reflection of a signal with its wavelength longer than the Bragg wavelength. The dependencies of the wavelength switching behaviors on various parameters of the mixed grating structure were demonstrated. Such results should be useful for optimizing the design of such a potentially useful fiber component.

OCIS codes: 050.2770, 060.2340.

Long-period fiber gratings have been considered for filtering applications in fiber communications[1−5]. It has been experimentally demonstrated that the combination of a long-period and a Bragg fiber gratings can result in the tunability of Bragg reflectivity and the switching of reflection wavelength[6,7]. Such a combination was implemented by applying an acoustic wave to a fiber Bragg grating for generating microbending. Because of the mixed coupling process of the long-period and Bragg gratings, the out-coupling of the core mode signal at the Bragg wavelength concurs with the signal coupling into the backward core mode from a cladding mode at a shorter wavelength. From the calculations of phase-matching conditions, the period of the long-period grating, i.e., the wavelength of the acoustic wave along the tapered fiber, could be calibrated[8]. Although the phase-matching conditions of such a mixed coupling process were identified, the coupling scenarios, particularly their dependencies on various device parameters, are still unclear.

In this letter, we demonstrated a novel numerical model for simulating the mixed coupling process. Based on this model, we could obtain the coupling results, quite similar to what observed experimentally[7]. Also, we discovered a novel mixed coupling process, which occurred at a wavelength longer than the Bragg wavelength. This is quite an unusual observation because conventionally a short-period fiber grating always results in cladding mode coupling at wavelengths shorter than the Bragg wavelength.

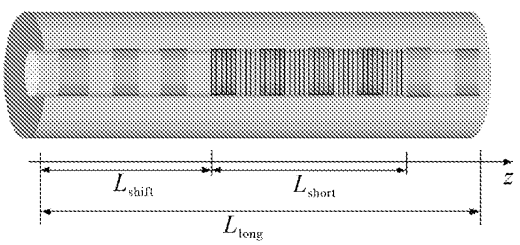

Fig. 1. Geometry of the mixed structure of a long-period and a Bragg fiber gratings.

The mixed structure of a long-period and a Bragg fiber gratings is schematically shown in Fig. 1. Here, L_{short} (Λ_{short}) and L_{long} (Λ_{long}) represent the lengths (periods) of the Bragg grating (called the short-period grating from now on) and the long-period grating, respectively. Also, L_{shift} stands for the relative position of the two gratings. In the mixture section, the refractive index of the fiber core is given by

$$n(z) = n_1 + \Delta n_{\text{short}}\left[1+\cos\left(\frac{2\pi z}{\Lambda_{\text{short}}}\right)\right] + \Delta n_{\text{long}}\left[1+\cos\left(\frac{2\pi z}{\Lambda_{\text{long}}}\right)\right], \quad (1)$$

here, n_1 is the unperturbed refractive index of the core, and Δn_{short} (Δn_{long}) is the refractive index fluctuation amplitude of the short-period (long-period) grating. It was assumed that the fiber jacket had been removed and the cladding was etched to a smaller size[7]. In numerical calculations, the general fiber parameter values were as follows. The refractive indices (radii) of the fiber core and cladding were 1.466 (4 μm) and 1.46 (15 μm), respectively. Also, $\Lambda_{\text{short}} = 0.53$ μm and $\Lambda_{\text{long}} = 340$ μm. Hence, the Bragg wavelength was 1541.5 nm.

To analyze the mode coupling process in such a mixed grating structure, we divided the whole grating structure into segments of ΔL in length such that $\Lambda_{\text{short}} \ll \Delta L \ll \Lambda_{\text{long}}$. In each segment, the optical wave experiences the periodically changing index due to the short-period grating and an approximately constant index offset due to the long-period grating. After some mathematical manipulations, the coupled equations in each segment were obtained as

$$\begin{aligned}\frac{\mathrm{d}A^{\text{co}}}{\mathrm{d}z} &= i\left\{K_{\text{L}}^{\text{co-co}} + k_{\text{S}}^{\text{co-co}}\right\}A^{\text{co}} \\ &+ i\sum_{\nu}\left\{K_{\text{L}\_\nu}^{\text{cl-co}} + k_{\text{S}\_\nu}^{\text{cl-co}}\right\}A_{\nu}^{\text{cl}}\mathrm{e}^{i[\beta_{\nu}^{\text{cl}}-\beta^{\text{co}}]z} \\ &+ i\left\{\frac{1}{2}k_{\text{S}}^{\text{co-co}}\mathrm{e}^{i\frac{2\pi}{\Lambda_{\text{short}}}z}\right\}B^{\text{co}}\mathrm{e}^{-i2\beta^{\text{co}}z} \\ &+ i\sum_{\nu}\left\{\frac{1}{2}k_{\text{S}\_\nu}^{\text{cl-co}}\mathrm{e}^{i\frac{2\pi}{\Lambda_{\text{short}}}z}\right\}B_{\nu}^{\text{cl}}\mathrm{e}^{-i[\beta_{\nu}^{\text{cl}}+\beta^{\text{co}}]z}, \quad (2a)\end{aligned}$$

$$\frac{\mathrm{d}B^{\mathrm{co}}}{\mathrm{d}z} = -i\left\{\frac{1}{2}k_{\mathrm{S}}^{\mathrm{co-co}}\mathrm{e}^{-i\frac{2\pi}{\Lambda_{\mathrm{short}}}z}\right\}A^{\mathrm{co}}\mathrm{e}^{i2\beta^{\mathrm{co}}z} - i\sum_{\nu}\left\{k_{\mathrm{S}\_\nu}^{\mathrm{cl-co}}\mathrm{e}^{-i\frac{2\pi}{\Lambda_{\mathrm{short}}}z}\right\}A_{\nu}^{\mathrm{cl}}\mathrm{e}^{i[\beta_{\nu}^{\mathrm{cl}}+\beta^{\mathrm{co}}]z} - i\left\{K_{\mathrm{L}}^{\mathrm{co-co}}+k_{\mathrm{S}}^{\mathrm{co-co}}\right\}B^{\mathrm{co}} - i\sum_{\nu}\left\{K_{\mathrm{L}\_\nu}^{\mathrm{cl-co}}+k_{\mathrm{S}\_\nu}^{\mathrm{cl-co}}\right\}B_{\nu}^{\mathrm{cl}}\mathrm{e}^{-i[\beta_{\nu}^{\mathrm{cl}}-\beta^{\mathrm{co}}]z}, \quad (2b)$$

$$\frac{\mathrm{d}A_{\nu}^{\mathrm{cl}}}{\mathrm{d}z} = i\left\{K_{\mathrm{L}\_\nu}^{\mathrm{cl-co}}+k_{\mathrm{S}\_\nu}^{\mathrm{cl-co}}\right\}A^{\mathrm{co}}\mathrm{e}^{i[\beta^{\mathrm{co}}-\beta_{\nu}^{\mathrm{cl}}]z} + i\left\{\frac{1}{2}k_{\mathrm{S}\_\nu}^{\mathrm{cl-co}}\mathrm{e}^{i\frac{2\pi}{\Lambda_{\mathrm{short}}}z}\right\}B^{\mathrm{co}}\mathrm{e}^{-i[\beta_{\nu}^{cl}+\beta^{\mathrm{co}}]z}, \quad \nu = 1,2,3,\cdots, \quad (2c)$$

$$\frac{\mathrm{d}B_{\nu}^{\mathrm{cl}}}{\mathrm{d}z} = -i\left\{\frac{1}{2}k_{\mathrm{S}\_\nu}^{\mathrm{cl-co}}\mathrm{e}^{-i\frac{2\pi}{\Lambda_{\mathrm{short}}}z}\right\}A^{\mathrm{co}}\mathrm{e}^{i[\beta_{\nu}^{\mathrm{cl}}+\beta^{\mathrm{co}}]z} - i\left\{K_{\mathrm{L}\_\nu}^{\mathrm{cl-co}}+k_{\mathrm{S}\_\nu}^{\mathrm{cl-co}}\right\}B^{\mathrm{co}}\mathrm{e}^{-i[\beta^{\mathrm{co}}-\beta_{\nu}^{\mathrm{cl}}]z}, \quad \nu = 1,2,3,\cdots, \quad (2d)$$

here, A^{co} and B^{co} are the complex amplitudes of the core mode with propagation constant β^{co}, and A_{ν}^{cl} and B_{ν}^{cl} are those of the νth cladding mode with propagation constant $\beta_{\nu}^{\mathrm{cl}}$, while A and B indicate the $+z$ and $-z$ propagation directions, respectively. Constants $K_{\mathrm{L}}^{\mathrm{co-co}}$ and $K_{\mathrm{L}\_\nu}^{\mathrm{cl-co}}$ are the coupling coefficients of the long-period grating and $k_{\mathrm{S}}^{\mathrm{co-co}}$ and $k_{\mathrm{S}\_\nu}^{\mathrm{cl-co}}$ are the coupling constants of the short-period grating[9]. By properly changing variables, we cast Eq. (2) into a set of simultaneous differential equations with constant coefficients, which could then be solved with the matrix method. The behaviors of the coupling process in this mixed grating were obtained by cascading the results of individual segments all together with appropriate boundary conditions. Note that the proposed numerical algorithms are quite general as long as the refractive index fluctuation amplitude is small and the condition $\Lambda_{\mathrm{short}} \ll \Delta L \ll \Lambda_{\mathrm{long}}$ is satisfied.

Figure 2 shows the 3-D illustration of the reflectivity dispersion of the mixed structure of various refractive index fluctuation amplitudes, Δn_{long}. To obtain these results, we used $L_{\mathrm{short}} = 35$ mm, $L_{\mathrm{long}} = 50$ mm and $\Delta n_{\mathrm{short}} = 1.9 \times 10^{-4}$, corresponding to the Bragg reflectivity of unity (at $\Delta n_{\mathrm{long}} = 0$) at wavelength 1541.5 nm. Also, the right end of the short-period grating coincided with that of the long-period one, i.e., $L_{\mathrm{shift}} = 15$ mm. In Fig. 2, one can see, besides the Bragg signal at 1541.5 nm, the emergence of two groups of reflected signals around 1539 and 1544 nm as Δn_{long} increases from zero. The wavelengths of these three groups of signals increase with Δn_{long}. This trend is due to the fact that the spatially averaged refractive index of the fiber core keeps increasing by the amount of $\Delta n_{\mathrm{short}} + \Delta n_{\mathrm{long}}$ (see Eq. (1)).

Similar observations of the emergence of the short-wavelength signal (1539 nm) were found in experiments[7]. However, the reflected long-wavelength

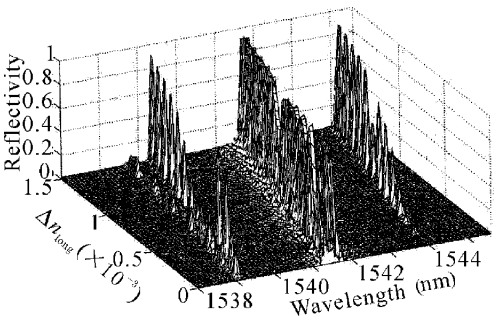

Fig. 2. 3-D illustration of the dispersive reflectivity variations of the mixed structure with the refractive index fluctuation amplitude, Δn_{long}.

signal (1544 nm) has never been reported. The intensities of such reflected signals and the Bragg reflectivity vary with Δn_{long}. It is interesting to note that the short-wavelength group splits into a strong and a weak signals. The wavelength of the strong signal red-shifts with that of the long-wavelength signal (1544 nm), indicating that they might be involved in the same coupling process. It can be shown that this is due to the simultaneous coupling among A^{co}, A^{cl} and B^{co} (or A^{co}, B^{cl} and B^{co}). By carefully examining Eq. (2), one can find the phase-matching conditions to be

$$2\beta^{\mathrm{co}} - \frac{2\pi}{\Lambda_{\mathrm{short}}} \pm \frac{2\pi}{\Lambda_{\mathrm{long}}} = 0, \quad (3)$$

where the positive (negative) sign corresponds to the long-wavelength (short-wavelength) signal. On the other hand, the appearance of the short-wavelength signal (around 1539 nm) may also result from the two-step coupling. First, the contra-directional coupling between A^{co} and B^{cl}, satisfying the phase-matching condition $\beta^{\mathrm{co}} + \beta^{\mathrm{cl}} - \frac{2\pi}{\Lambda_{\mathrm{short}}} = 0$, through the short-period grating occurs. Second, the co-directional coupling between B^{cl} and B^{co}, roughly satisfying the phase-matching condition $\beta^{\mathrm{co}} - \beta^{\mathrm{cl}} - \frac{2\pi}{\Lambda_{\mathrm{long}}} = 0$, through the long-period grating follows. Since the second coupling process can occur in quite a wide bandwidth, the resultant coupling wavelength is essentially determined by the first coupling process. This phenomenon has already been observed in experiments[7] and discussed in Ref. [8]. Therefore, the short-wavelength signal around 1539 nm stems from two different mode-coupling mechanisms, which happen to occur at the same wavelength for small Δn_{long}. However, as Δn_{long} becomes large, the short-wavelength group splits into two signals corresponding to the two mode-coupling mechanisms, as shown in Fig. 2. Between the two signals, the strong one is generated with the phase-matching condition in Eq. (3) (with the negative sign).

The variations of the Bragg reflectivity and the short-wavelength signal simulate a wavelength switching process, as experimentally shown in Ref. [7]. Figure 3 highlights the switching process with the data extracted from Fig. 2. Here, the three curves represent the cases of $\Delta n_{\mathrm{long}} = 1.3 \times 10^{-4}$, 1.5×10^{-4} and 1.8×10^{-4}, corresponding to different acoustic intensities on the fiber in the experiments[7]. Although the conditions are not exactly the same, Fig. 3 does demonstrate the same trend.

To further understand the characteristics of the mixed grating structure, Fig. 4 shows the variations of reflectivity of the aforementioned three signals with the relative position L_{shift}. In these calculations, we increased L_{long} to 120 mm and fixed Δn_{long} at 1.8×10^{-4}. The rest of parameters were the same as those for Fig. 2. With such a small value of Δn_{long}, the reflectivity of the long-wavelength signal was quite small. One can see that as L_{shift} increases, the reflectivity levels of the Bragg and short-wavelength signals vary periodically with slightly different periods and phases. Then, Fig. 5 shows the reflectivity variations in varying L_{long}. Here, L_{short} was fixed at 35 mm and the right end of the short-period grating coincided with that of the long-period one. The rest of parameters were the same as those for Fig. 4. Again, we can see the almost perfectly periodical variations of the Bragg and short-signal reflectivity levels. Since the coupling phenomena are in periodical nature, the observed periodical variations are quite reasonable. From the similarity between Figs. 4 and 5, one can conclude that the part of the long-period grating after the mixture section had little effect on the reflectivity spectrum. Plotted in Fig. 6 are the reflectivity variations with L_{short}. Here, the periodical nature is not quite clear. In this case, L_{long} was fixed at 50 mm and the right end of the short-period grating coincided with that of the long-period one, so L_{shift} was also varied. The results in Figs. $4-6$ could provide us useful design information for a practical component.

In summary, we have proposed a numerical model for evaluating the coupling processes of a mixed structure

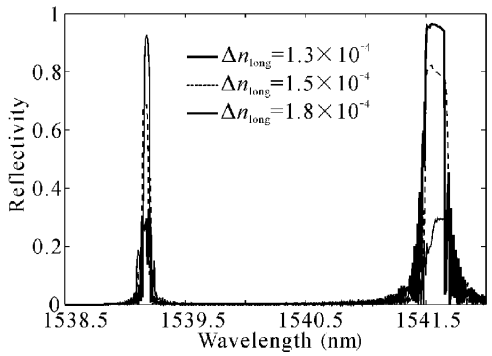

Fig. 3. Wavelength switching behaviors with the data extracted from Fig. 2.

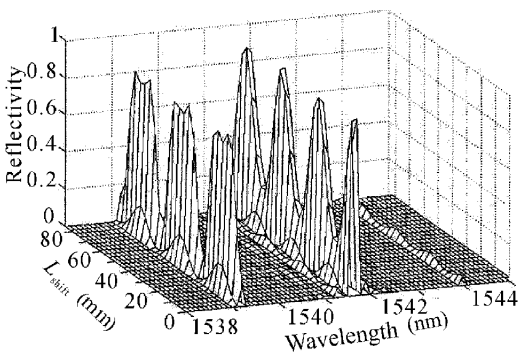

Fig. 4. Variations of reflectivity of the three signals with the relative position, L_{shift}.

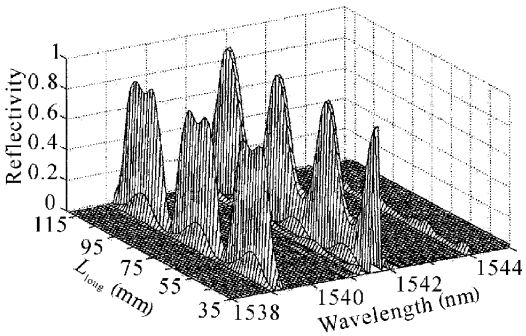

Fig. 5. Variations of reflectivity of the three signals with the length of the long-period grating, L_{long}.

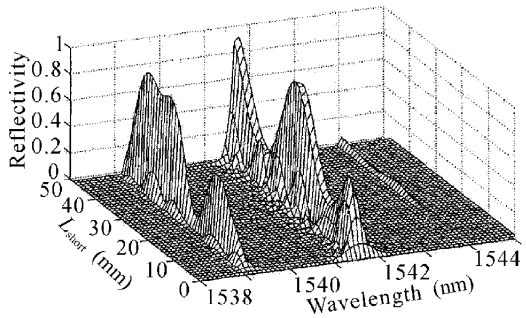

Fig. 6. Variations of reflectivity of the three signals with the length of the short-period grating, L_{short}.

of a Bragg fiber grating and a long-period grating. From the numerical results, we not only confirmed the wavelength switching phenomena observed in experiments, but also discovered a new coupling mechanism, which generated the reflection of a signal with its wavelength longer than the Bragg wavelength. The dependencies of the wavelength switching behaviors on various parameters of the mixed structure were demonstrated. Such results should be useful for optimizing the design of such a potentially useful fiber component.

This research was supported by National Science Council, under the grants of NSC 90-2215-E-002-029, NSC 90-2112-M-002-052, NSC 90-2215-E-002-027, and NSC 90-2215-E-002-041. C. C. Yang is to whom the correspondence should be addressed, his e-mail address is ccy@cc.ee.ntu.edu.tw.

References

1. B. Y. Kim, *et al.*, Opt. Lett. **11,** 389 (1986).
2. A. M. Vengsarkar, *et al.*, IEEE J. Lightwave Technol. **14,** 58 (1996).
3. W. F. Liu, *et al.*, IEEE J. Lightwave Technol. **16,** 2006 (1998).
4. R. Feced, *et al.*, IEEE J. Select. Topics Quantum Electron. **5,** 1278 (1999).
5. S. Savin, *et al.*, Opt. Lett. **25,** 710 (2000).
6. D. W. Huang, *et al.*, IEEE Photon. Technol. Lett. **12,** 176 (2000).
7. W. F. Liu, *et al.*, Opt. Lett. **25,** 1319 (2000).
8. N. H. Sun, *et al.*, IEEE J. Lightwave Technol. **20,** 311 (2002).
9. T. Erdogan, J. Opt. Soc. Am. A, **14,** 1760 (1997).